Vermessung & Geoinformation 2/2024, pp. 54 – 62, 8 Figs.

Wave Height Determination Based on Low-Cost Inertial Measurements Units: Potential and Challenges for an Innovative Environmental Monitoring System

Wellenhöhenbestimmung auf der Basis von kostengünstigen inertialen Messeinheiten: Potenziale und Herausforderungen für ein innovatives Umweltüberwachungssystem

Karin Mascher and Philipp Berglez, Graz

Abstract

The quantity of aquatic plants and subsequent biodiversity at Lake Wörthersee, Carinthia's largest lake, is showing a declining trend. Local aquatic ecologists suggest that the rising boat traffic on the lake might be one of the reasons behind this decline. Increased wave action at the shore leads to the stirring up of more sludge particles, disturbing plant growth and causing a corresponding reduction in biodiversity. To address this research question, capturing the energy emitted by passing boats and the energy reaching the shore is crucial; with key parameters being wave height and wave period.

This study conducted test measurements at Lake Wörthersee to demonstrate the capability of buoys equipped with low-cost inertial sensors in capturing wave heights. While showcasing their potential, the study also addresses the challenges involved. To validate the obtained results, comparisons were made with reference measurements obtained from a total station. Additionally, the study presents an approach aimed at distinguishing boat-induced waves from wind-induced waves using the wavelet transform.

Keywords: inertial measurement unit, trend determination, wavelet transform

Kurzfassung

Der Bestand an Wasserpflanzen und die damit verbundene Artenvielfalt des Wörthersees in Kärnten nimmt stetig ab. Ein möglicher Grund dafür könnte, laut örtlichen Gewässerökologen, der steigende Bootsverkehr am See sein. Erhöhte Wellenaktivität am Ufer führt dazu, dass mehr Schlammteilchen aufgewirbelt werden, was das Pflanzenwachstum stört und zu einer entsprechenden Verringerung der Biodiversität führt. Um diese Forschungsfrage beantworten zu können, muss die von den vorbeifahrenden Booten ausgehende und die am Ufer eintreffende Energie gemessen werden; wichtige Parameter sind dabei die Wellenhöhe und -periode.

Basierend auf Testmessungen am Wörthersee wird das Potential von Messbojen, welche mit kostengünstiger Inertialsensorik ausgestattet sind, zur Erfassung von Wellenhöhen aufgezeigt. Die damit verbundenen Herausforderungen werden ebenfalls angesprochen. Zur Validierung der Ergebnisse wurden Referenzmessungen mittels einer Totalstation durchgeführt. Darüber hinaus wird ein Ansatz vorgestellt, der darauf abzielt, mithilfe der Wavelet-Transformation, Boots- von Windwellen zu unterscheiden.

Schlüsselwörter: inertiale Messeinheit, Trendbestimmung, Wavelet-Transformation

1. Introduction

The ecological condition and quality of Lake Wörthersee (Carinthia/Austria) worsens increasingly over time [1]. Certain aquatic plants, and thus the biodiversity, are falling, which alarms local aquatic ecologists. One assumption is that boat traffic may be related to the extinction of plant species.

Waves are hitting the shore and stir up fine sludge particles and sediments. These, in turn, settle on the aquatic plants. If the sludge layer becomes too thick, aquatic plants cannot carry out photosynthesis leading to dying [1]. A key research question is whether, and if so, how strongly – aquatic plants are affected by wave action and, thus, if boat traffic represents an environmental threat.

Hence, the determination of wave heights and periods gives valuable information about wave action at the lake. Wave heights and periods are determinable by several effective methods. One way is to analyze the signal-to-noise ratio signal of Global Navigation Satellite System (GNSS) reflectometry to obtain wave heights [2]. Another

possibility represents GNSS buoys using precise point positioning (PPP) [3,4]. Although PPP provides centimeter accuracy, such systems are cost-intensive and do not take into account the changing attitude of a buoy at sea [5].

Other studies determine wave parameters based on micro-electro-mechanical system (MEMS) inertial measurement units (IMUs) attached to buoys [6,7]. An IMU is characterized by its high output rate and its high short-time stability – but low long-time stability. Thus, the main issue concerning IMU data processing refers to the mitigation of the accumulation of sensor errors [8], which results in a drift. Typically, when integrating an INS, other systems, such as GNSS, or mathematical methods are used for aid. By coupling GNSS with INS, missing attitude information is incorporated into the processing, and thus, the solution can be significantly improved [5]. Zhang et al. [6] propose a method for measuring wave heights and periods only using a MEMS IMU. They utilized frequency domain integration methods to transform the detrended and denoised acceleration data to wave heights and periods. Simulating wave eigenvalues using a sinusoidal simulation mechanism showed that statistical wave properties are accurately extractable. A master's thesis from Alfens [7] deals with the IMU-based sea state estimation using machine learning methodologies for vessels. He presents a robust algorithm but also addresses the difficulties connected to the real-life dynamics of a vessel.

Numerous methods for determining wave characteristics are often costly, impractical, reliant solely on simulations, or tailored exclusively for oceanic environments. Thus, to date, such measurement buoys have not been applied in contexts related to lake ecosystems. A primary objective is to evaluate the feasibility of extracting wave heights utilizing a conventional strap-down algorithm along with advanced data processing techniques to detrend and denoise the time series.

The trend determination process involves two phases: the initial phase focuses on trend elimination via moving averages, while the subsequent phase utilizes methods of local regression to eliminate residual trends. Wavelet methodologies are then employed to denoise distorted segments, integrating neighboring coefficients. This denoising process aims to filter out wind-induced waves, leaving behind only boat-generated waves. One of the primary challenges involves coping with fluctuating temperatures throughout the day while accurately capturing wave heights that are mere centimeters in magnitude. To validate this approach, a field test was conducted at Lake Wörthersee, outfitting a total of eight buoys with MEMS IMUs. One buoy was tracked using a total station to verify the developed algorithm.

This paper is divided into three sections: Section 2 delineates the methodologies employed, the selected sensor, and details regarding the measurement campaign. Section 3 focuses on presenting the results obtained. The final Section 4 concludes the paper by providing a summary as well as a discussion.

2. Materials and Methods

The following sections introduce the selected MEMS IMU for measuring wave heights and give an overview of the analysis methods. Furthermore, the field measurement is described.

2.1 Selected Sensors

Inertial data samples of MEMS IMUs are collected via the XSens Dots [9] from the company XSens. The XSens DOT is composed of a triaxial accelerometer, a triaxial gyroscope, and a triaxial magnetometer, which measures accelerations, angular rates, and magnetic field strength, respectively. With its dimensions of 36.30 x 30.35 x 10.80 mm, output rates up to 120 Hz, battery life of up to 9 hours, and internal storage of 64 MB, it features a wearable sensor suitable for many applications. The sensor's bias instability, which denotes the extent of sensor output drift over time under consistent operating conditions and steady temperature, is relatively high at 10°/h, thus, impacting its stability and reliability during operation. Nonetheless, given the focus solely on short-term changes, this level of stability proves sufficient.

2.2 Definition of wave height and period

The wave heights are defined for up-crossing waves. The wave period refers to the crest period, thus, the time span between an up-crossing and the next down-crossing is measured. The definitions are illustrated in Figure 1. Those statistical values can be extracted via the WAFO (Wave Analysis for Fatigue and Oceanography) toolbox for Python [10].

2.3 Strapdown Integration

The parameter of interest in this study is the relative height component, which is computed via the conventional strap-down integration. Thus, inertial

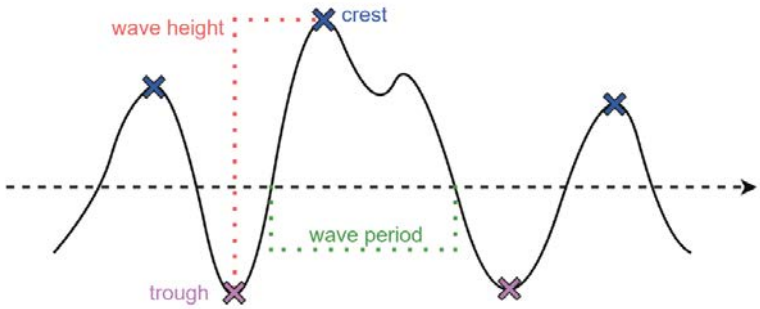

Fig. 1: Definition of wave height and period

data (accelerations f^b and angular rates Ω_{ib}^b) are converted into relative position/velocity/attitude (PVA) changes. The used mechanization equation reads as follows [11,12]:

$$\begin{bmatrix} \dot{\boldsymbol{x}}^l \\ \dot{\boldsymbol{v}}^l \\ \dot{\boldsymbol{R}}_b^l \end{bmatrix} = \begin{bmatrix} \boldsymbol{v}^l \\ \boldsymbol{R}_b^l \boldsymbol{f}^b - (2\boldsymbol{\Omega}_{ie}^l + \boldsymbol{\Omega}_{el}^l)\boldsymbol{v}^l + \overline{\boldsymbol{g}}^l \\ \boldsymbol{R}_b^l(\boldsymbol{\Omega}_{ib}^b - \boldsymbol{\Omega}_{il}^b) \end{bmatrix} \quad (1)$$

where $\boldsymbol{x}^l$ contains the position in the local-level frame (l-frame). The definition of the axes of the l-frame corresponds to an east-north-up system. The vector $\boldsymbol{v}^l$ is the velocity vector, where the normal gravity vector $\overline{\boldsymbol{g}}^l$ [13] and the Coriolis part $(2\boldsymbol{\Omega}_{ie}^l + \boldsymbol{\Omega}_{el}^l)v^l$ are taken into account. $\boldsymbol{R}_b^l$ is the rotation matrix that transforms a vector from the body frame (b-frame) to the l-frame. The rotation matrix is parameterized by quaternions to increase the numerical stability. Basically, $\boldsymbol{\Omega}$ is associated with a skew-symmetric cross-product matrix, where, e.g., $\boldsymbol{\Omega}_{ib}^b$ corresponds to the skew-symmetric matrix containing the angular rate vector. A more detailed description can be found in Mascher et al. [14]. Integrating the mechanization equation based on the rectangular rule yield the desired states. Note that the raw acceleration measurements are corrected by pre-determined acceleration biases and scale factors. The gyroscope bias is calculated in the initialization process, and in parallel with the initial alignment, where the initial roll and pitch values are computed based on the accelerometer data. The initial heading is derived from magnetometer data. The initial position, as well as the initial velocity vector, are the null vector.

Despite the pre-calibration process of the IMU, other deterministic and cumulative stochastic sensor errors are present, which results in a rapid drift of the INS position solution [15]. The major environmental factor is varying temperature conditions. Its modeling presents a time-consuming process. However, in post-processing, the drift of the IMU can be eliminated by time series analysis to a large extent. Alignment errors are another challenge for a standalone INS. Primarily, tilt errors and heading errors cause a miscalculation of the gravitational component. As a result, the Schuler oscillations (84.4 minute cyclic responses) are evoked [16].

2.4 Filtering

The filtering procedure consists of two main steps: The first one deals with the trend (drift) elimination of the INS height solution. The second one focuses on denoising the signal to extract wave heights that are associated with boat traffic.

2.4.1 Trend determination

An iterative process determines the trend, where different trend determination methods are considered:

As a first step, an initial trend (main drift) is determined using a centered moving average of the time series based on a 1-D convolution filter. As window length, 45 samples are chosen, which corresponds to 1.5 s of inertial data. After removing this initial trend, a more sophisticated method, namely Seasonal-Trend decomposition using locally weighted regression (LOESS), or in abbreviated form “STL” [17], is used for determining the remaining trend. According to Cleveland et al. [17], STL is an advanced filtering method that divides the signal into a trend, seasonal, and remainder (noise) component. Mainly, it is based on iteratively adjusting local regression models. The seasonal component is neglected and only the trend is again subtracted from the time series.

2.4.2 Wavelet Transform

One popular frequency analysis/filtering tool represents the Fast Fourier Transform (FFT). This

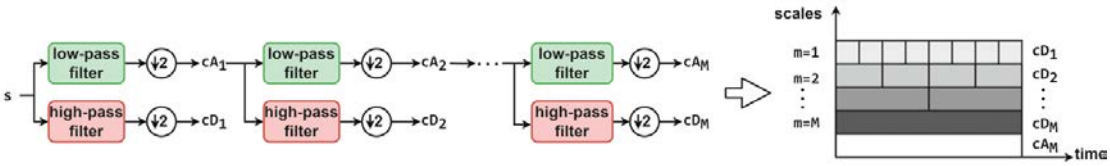

Fig. 2: Multiresolution signal decomposition and transform plot with scale indexing

approach is well suited for stationary time series. However, for non-stationary signals, which vary strongly over time, the FFT causes difficulties. Another issue that plays a central role in this study is that waves caused by wind show similar frequency characteristics to waves caused by boats. Thus, if the noise is within the desired spectral content, Fourier filters fail to work. The Wavelet Transform (WT) resolves these limitations. For the WT, the signal is correlated with so-called wavelets, which represent shifted and scaled versions of the mother wavelet ψ. The WT of a continuous signal $s(t)$ reads as follows [18,19]:

$$T(a,b) = \langle s, \psi_{a,b} \rangle = \int_{-\infty}^{\infty} s(t) \psi_{a,b}^{*} \, dt, \qquad (2)$$

where a and b are the dilation and translation parameters, respectively. The complex conjugate of the scaled and shifted wavelet is denoted as $\psi_{a,b}^{*}$. By discretizing the dilatation and translation parameters, the discrete wavelet transform (DWT) is obtained:

$$T(m,n) = \langle s, \psi_{m,n} \rangle, \qquad (3)$$

where m and n are the corresponding control parameters for the dilation and translation.

In 1998, Mallat [20] introduces the theory for fast wavelet decomposition and reconstruction algorithms using a wavelet orthonormal basis yielding to the fast wavelet transform (FWT). His idea of the multiresolution signal decomposition is based on the pyramid algorithm that utilizes quadrature mirror filters. The implementation can be interpreted as a cascade of high-pass and low-pass filters based on the discrete wavelet transform (DWT): A finite signal s can be decomposed into so-called approximation coefficients cA_1 and detail coefficients cD_1 ,by applying low-pass and high-pass filtering, respectively, followed by dyadic decimation. These coefficients refer to the first level of decomposition at the scale index $m = 1$. The filtering process (Figure 2) is repeated for the approximation coefficients until the desired level m or the maximum level M of decomposition is reached ($0 < m < M$).

The bandwidths at each scale m are equal to

$$\left[\frac{f_s}{2^{m+1}}, \frac{f_s}{2^m} \right] \qquad (4)$$

for cD_m and

$$\left[0, \frac{f_s}{2^{m+1}} \right] \qquad (5)$$

for cA_m [21]. f_s denotes the sampling frequency.

As also seen in Figure 2, the resulting dyadic grid wavelet transform coefficients yield a 2D discrete transform plot, which gives an impression of the frequency distribution. High frequencies refer to small scales and provide a high time resolution and low frequency resolution. Conversely, high scales are associated with low frequencies, which have a low time resolution, but a high frequency resolution.

Similarly, the discrete signal is reconstructed with the pyramid transform, also known as the inverse Fast Wavelet Transform (IFWT). Taking cA_m and cD_m, the original signal is reconstructed by inverting the pyramid algorithm [20].

2.4.3 Wavelet Denoising

Wind and heavy boat traffic are potential sources of interference. They result in a superposition of the individual waves, thus, outgoing energy from single boats is hardly identifiable. By denoising the signal, the distorted parts are minimized, and the determination of wave heights and periods is facilitated.

Wavelet denoising consists of the following parts:

- **Decomposition**: Decompose signal into multiple frequency bands using the FWT.
- **Thresholding**: Reduce the relative importance of transform coefficients with low absolute values.
- **Reconstruction**: Reconstruct the signal from the denoised coefficients using the FIWT.

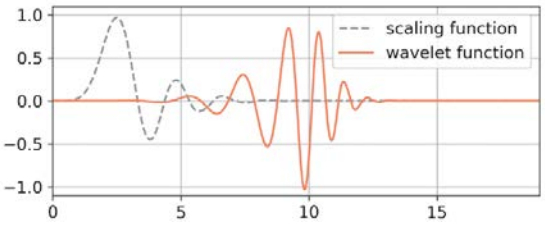

Fig. 3: Daubechies' wavelets with ten vanishing moments

Standard approaches use hard or soft thresholding functions, which are applied to each wavelet coefficient, to denoise a signal. However, Cai and Silverman [22] proposed an advanced denoising method called the *"NeighBlock"*. This approach includes information on neighboring coefficients in overlapping blocks (block thresholding) in the decision-making. The basic assumption of block thresholding is that if some coefficients contain a signal, it is likely that coefficients in the near vicinity also have some information.

The chosen wavelet for denoising the signal is the Daubechies' wavelet with ten vanishing moments (Figure 3).

2.5 Field Tests

Field tests were conducted at the Lake Wörthersee on 31. July 2022 between 06:30 and 18:00. Therefore, eight buoys and three anchor buoys were well-placed south of the "Schlangeninsel". The test setup is sketched in Figure 4.

The anchor buoys are positioned 100 meters apart from one another forming a L-shape. Secured with velcro fasteners, one IMU was attached centrally to each yellow buoy. However, a central attachment of the IMU for the number one buoy, the orange one, was not possible, since this buoy was additionally equipped with a Leica GRZ101 360-degree Mini Prism. From the shore, the prism was tracked using a Leica Nova MS60 MultiStation to obtain a reliable ground truth for selected periods. The IMU data was recorded and stored within the sensor's internal storage at 30 Hz. Due to the limited battery life of each sensor (up to 9 hours @ 30 Hz), the IMUs were exchanged shortly before 14:00. Since it cannot be assumed that the buoys in the lake are stationary, the initialization process of the IMU was done on land. After a successful initial alignment, the buoys were reached by boat to attach the sensors.

The morning session focused on individual boat trips. From 07:15 until 08:30 single boats up

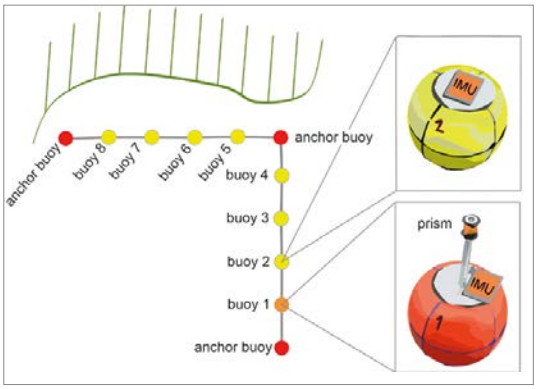

Fig. 4: Test setup. The distance between the buoys measures roughly 20 m. Buoy 1 was additionally equipped with a Leica 360° mini prism.

to 7.3 m in length were passing by the buoys to obtain an isolated data set. This session featured still air atmospheric conditions. After 10 o'clock more boat traffic and the rising wind were present. In the afternoon, gusts of winds were sensed occasionally. Under sunny weather conditions, the temperature range was approximately between 17 °C and 27 °C on land. Due to the strong solar radiation on the water, the sensor experienced higher temperatures.

3. Results

This section presents the final and intermediate results of the wave height determination. By comparing the INS solution with the reference, meaningful results and evaluations can be obtained.

3.1 Trend Elimination

As seen in Figure 5, the pure strapdown integration results in a rapid drift in the PVA. Due to tilting as well as sensor errors of the MEMS IMU, the Schuler oscillation (~84 min) becomes visible. Since the INS shows great short-time stability, height information can be obtained by detrending the time series in post-processing. After subtracting the initial trend (moving average) from the original time series, several small trends remain. Those trends are likely a result of temperature changes and tilting errors. However, after applying the STL analysis, wave heights are noticeable.

3.2 Comparison with reference

Figure 6 indicates an example of waves that originates from a passing boat (Super Air Nautique Gs 22) for all buoys. The arrangement of the buoys

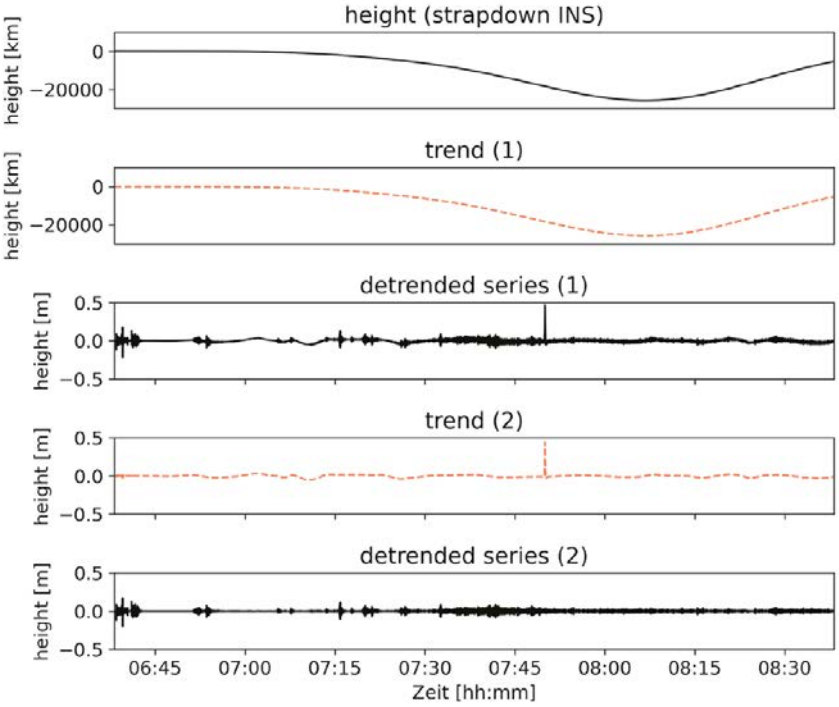

Fig. 5: Trend elimination. Trend (1) refers to the moving average, trend (2) to STL.

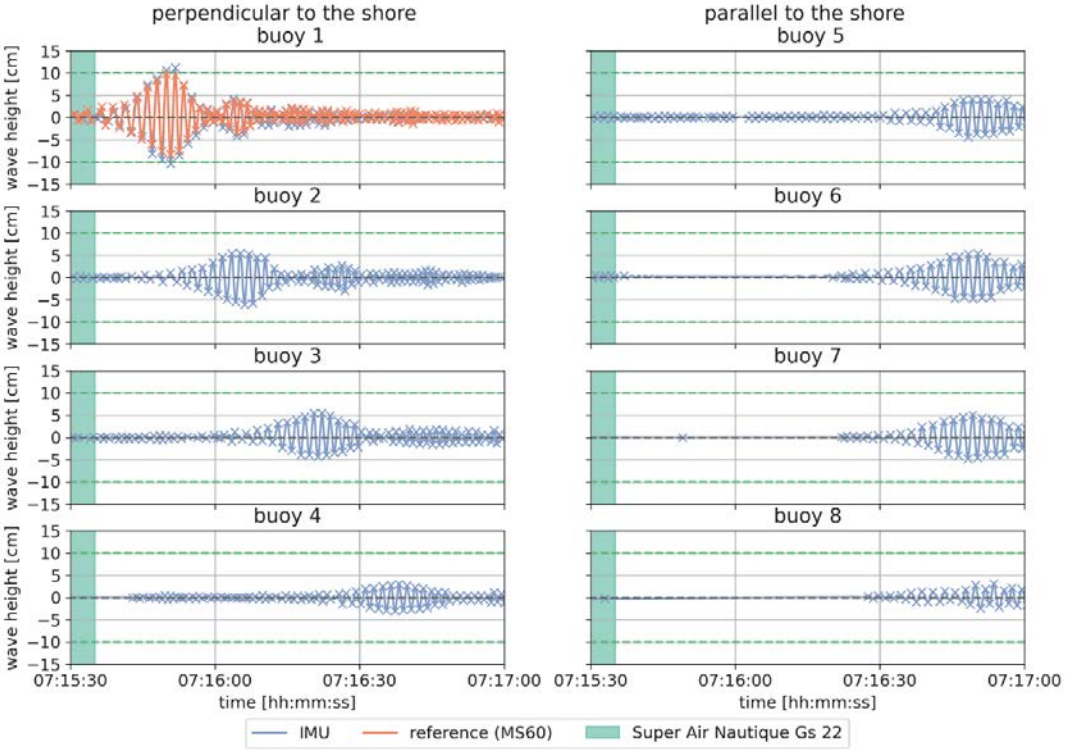

Fig. 6: Computed wave heights. The detail shows the transmitted energy based on the Super Air Nautique Gs 22, a boat with a length of 6.7 m. The cyan patch indicates the transit time of the boat near the buoys.

is illustrated in Figure 4. The signal refers to the detrended time series obtained by the inertial data. The wave reaches the buoys, which are perpendicular to the shore, with decreasing energy and delay. Since the parallel aligned buoys are close to the shore, the waves regain height. The wave height of buoy one matches the measured reference within 7 mm. However, this example shows the result under perfect conditions (no wind, no other boat traffic).

In Table 1, the average root-mean-square errors (ARMSEs) of buoy number one are listed. Conditions, like no wind and nearly no boat traffic, result in low ARMSE values. Rising wind and boat traffic cause more movement on the water's surface, thus, independent waves are superimposed. The buoy is tilted heavily, which results in higher ARMSE values around 4 cm. However, the ARMSE values should be interpreted with care since the prism and IMU are not affected identically by incoming waves due to their different mountings.

reference	*conditions*	*ARMSE* [cm]	*time span*
1	nearly no wind nearly no boat traffic	1.5	07:10 08:30
2	rising wind rising boat traffic	2.1	09:15 11:15
3	heavy wind heavy boat traffic	4.3	12:07 13:45
4	heavy wind heavy boat traffic	3.0	14:15 16:10

Tab. 1: Average root-mean-square error (ARMSE) of the height component

Scale Index	*Frequency range* [Hz]	
$m=4$	0.94	1.88
$m=5$	0.47	0.94
$m=6$	0.22	0.47

Tab. 2: Frequency ranges corresponding to decomposition levels of interest. The sampling rate is 30 Hz.

3.3 Frequency Analysis

Since wind and heavy boat traffic are potential sources of interference, the signal is denoised based on wavelet methodologies. The goal is to isolate waves that originate from boats and are not affected by wind. That data shall serve as the basis for the determination of wave periods and wave heights. In one initial approach, a discrete transform plot of the detrended time series (Figure 7) over the entire measurement day is analyzed.

Wave energy is transmitted between 0.2 and 1.9 Hz (Formula (4)). The context between the scales and sub-frequency bands is stated in Table 2.

However, the signal is still distorted by wind waves that are in a similar frequency band to waves caused by boats. By denoising the signal with the *"NeighBlock"*

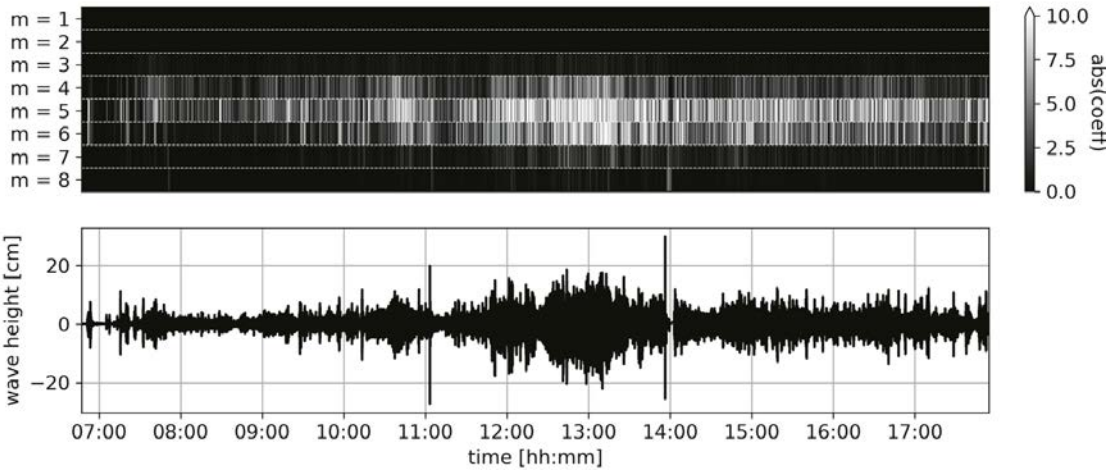

Fig. 7: Discrete transform plot with scale indexing of one selected buoy. Note that the IMU was exchanged shortly before 14:00 o'clock.

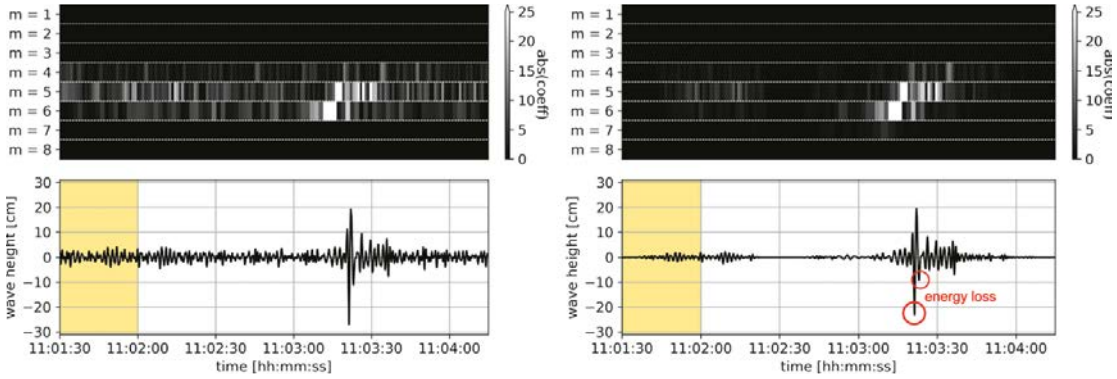

Fig. 8: Wave caused by ferry. The yellow patch indicates the approximate transit time of the ferry near the buoys. Noisy signal (left). Denoised signal (right).

method based on the Wavelet Daubechies 10, the wave can be highlighted. The assumption is that waves caused by wind yield less energy than waves, which are a result of passing boats. Hence, the relative importance of coefficients with low energy is decreased. Figure 8 compares the noisy signal with the denoised one caused by a ferry, which passed the buoys during windy conditions. The distorted parts could be minimized. Nevertheless, there is also a slight decrease in amplitude, notably concerning the troughs by a few millimeters. To improve/calibrate the filtering methods, further information, such as wind speed and direction would be needed.

4. Conclusion and Discussion

Since IMUs have great short-time stability, a stand-alone INS can determine wave heights through advanced data processing. Different trend determination methods are applied to eliminate the drift. A comparison of the INS with reference measurements of a total station showed that wave heights, under good conditions, are determinable within 1 cm. However, when the waves get rough out on the lake due to wind or heavy boat traffic, the accuracy degrades. Distorted parts, which are a result of wind and noise, are filtered by wavelets. The methodology for wavelet denoising is based on the assumption that waves caused by wind contain less significant energy than waves caused by passing boats. Wave heights and periods of specific events can be further extracted using, e.g., the WAFO toolbox [10]. The propagation of wave heights and periods yields valuable information that can be extended to other areas of Lake Wörthersee through models and simulations. The required accuracy for these models should not surpass five centimeters, a requirement that the proposed approach successfully met.

Although the MEMS IMU sensed inertial data over several hours, tilting errors due to inaccurate initialization seem to have no substantial impact on the height determination. In part, this could be in recognition of the fact that waves are based on harmonic movements.

However, these results are based on an initial feasibility study, and further information and measurement campaigns are required to establish a scientifically supported statement regarding whether boat traffic correlates with the decreased biodiversity in Lake Wörthersee. Despite encountering various challenges, including tilting errors, temperature gradients, and wind, it has been demonstrated that MEMS IMUs hold significant potential in accurately capturing wave energy. Moreover, these low-cost measurement buoys exhibit high scalability, enabling a broad spectrum of applications.

Consequently, the research project WAMOS (WAve MOnitoring System) was initiated in October 2023. The primary objective of this project is to develop an interdisciplinary monitoring system that analyzes and links together wave heights, boat traffic, meteorology, sediment content, and macrophyte vegetation. This investigation seeks to understand the impact of boat traffic on vegetation and to identify necessary countermeasures, such as wave protection measures. Therefore, an integral aspect involves enhancing the measurement buoys, including the integration of the free-of-charge Galileo High Accuracy Service and capturing wave heights in near-real-time.

Acknowledgement

Many thanks to the Institute of Hydraulic Engineering and Water Resources Management (Graz University of Technology), especially Univ.-Prof. Gerald Zenz, for the cooperation and support during this feasibility study. Thanks to the Carinthian Institute for Lake Research for initializing and supporting this study.

Together with the Institute of Hydraulic Engineering and Water Resources Management (Graz University of Technology), the SIENA research group (Carinthia University of Applied Sciences), Systema Bio- and Management Consulting GmbH, Ingenieurgesellschaft Prof. Kobus und Partner GmbH, and the Carinthian Institute for Lake Research, the Working Group of Navigation from the Institute of Geodesy (Graz University of Technology) is currently conducting further investigations and developing a wave monitoring system within the scope of the research project "WAMOS". The project "WAMOS" is funded by the Austrian Promotion Agency (FFG) within the "Austrian Space Application Programme (ASAP)".

References

[1] kaernten.ORF.at. Wasserpflanzensterben wird erforscht. Available online: https://kaernten.orf.at/stories/3167158/ (accessed on 3 October 2022).

[2] *Roggenbuck, O.; Reinking, J.; Lambertus, T.*: Determination of Significant Wave Heights Using Damping Coefficients of Attenuated GNSS SNR Data from Static and Kinematic Observations. Remote Sensing 2019, 11, doi:10.3390/rs11040409.

[3] *Zhu, L.; Yang, L.; Xu, Y.; Yang, F.; Zhou, X.*: Retrieving Wave Parameters From GNSS Buoy Measurements Using the PPP Mode. IEEE Geoscience and Remote Sensing Letters 2022, 19, 1–5, doi:10.1109/LGRS.2020.3041846.

[4] *F. Fund; F. Perosanz; L. Testut; S. Loyer.*: An Integer Precise Point Positioning technique for sea surface observations using a GPS buoy. Advances in Space Research 2013, 51, 1311–1322, doi:10.1016/j.asr.2012.09.028.

[5] *Zhou, B.; Watson, C.; Legresy, B.; King, M.A.; Beardsley, J.; Deane, A.*: GNSS/INS-Equipped Buoys for Altimetry Validation: Lessons Learnt and New Directions from the Bass Strait Validation Facility. Remote Sensing 2020, 12, doi:10.3390/rs12183001.

[6] *Zhang, Y.; Qi, L.; Dong, J.; Wen, Q.; Lv, M.*: Data Processing Based on Low-Precision IMU Equipment to Predict Wave Height and Wave Period. In 2019 2nd International Conference on Data Intelligence and Security (ICDIS). 2019 2nd International Conference on Data Intelligence and Security (ICDIS), South Padre Island, TX, USA, 28/06/2019–30/06/2019; IEEE, 2019–2019; pp 103–107, ISBN 978-1-7281-2080-5.

[7] *Jens Nikolai Alfsen*: IMU-based sea state estimation using IMU-based sea state estimation using convolutional neural networks for DP vessels; Norwegian University of Science and Technology, Trondheim, Norway, 2020.

[8] *Ren, M.; Pan, K.; Liu, Y.; Guo, H.; Zhang, X.; Wang, P.*: A Novel Pedestrian Navigation Algorithm for a Foot-Mounted Inertial-Sensor-Based System. Sensors 2016, 16, 1–13, doi:10.3390/s16010139.

[9] Xsens DOT User Manual, Document XD0502P, Revision D. Available online: https://www.xsens.com/xsens-dot.

[10] WAFO group. WAFO – a Matlab Toolbox for Analysis of Random Waves and Loads: Tutorial for WAFO version 2017, 2017.

[11] *Noureldin, A.*: Fundamentals of Inertial Navigation, Satellite-based Positioning and their Integration; Springer: Berlin, Heidelberg, 2013, ISBN 978-3-642-30465-1.

[12] *Hofmann-Wellenhof, B.; Legat, K.; Wieser, M.*: Navigation: Principles of Positioning and Guidance; Springer Vienna: Vienna, s.l., 2003, ISBN 978-3-7091-6078-7.

[13] *Vajda, P.; Panisova, J.*: Practical comparison of formulae for computing normal gravity at the observation point with emphasis on the territory of Slovakia. Contributions to Geophysics and Geodesy 2005, 35, 173–188.

[14] *Mascher, K.; Wieser, M.*: Foot-Mounted Inertial Navigation – Implementation and Fusion Concept into a Bayesian Filtering Framework. In 2021 International Conference on Indoor Positioning and Indoor Navigation (IPIN).

[15] *Altinoz, B.; Unsal, D.*: Determining efficient temperature test points for IMU calibration. In 2018 IEEE/ION Position, Location and Navigation Symposium (PLANS). 2018 IEEE/ION Position, Location and Navigation Symposium (PLANS), Monterey, CA, 23/04/2018–26/04/2018; IEEE, 2018–2018; pp 552–556, ISBN 978-1-5386-1647-5.

[16] *Grewal, M.S.*: Global positioning systems, inertial navigation, and integration, 2nd ed.; Wiley-Interscience: Hoboken, N.J., 2007, ISBN 978-0-470-04190-1.

[17] *Cleveland, R.B.; Cleveland, W.S.; Terpenning, I.*: STL: A Seasonal-Trend Decomposition Procedure Based on Loess. Journal of Official Statistics 1990, 6, 3.

[18] *Addison, P.S.*: The illustrated wavelet transform handbook: Introductory theory and applications in science, engineering, medicine and finance, Second edition; CRC Press Taylor & Francis Group: Boca Raton, Fla., 2017, ISBN 1482251329.

[19] *Rhif, M.; Ben Abbes, A.; Farah, I.; Martínez, B.; Sang, Y.*: Wavelet Transform Application for/in Non-Stationary Time-Series Analysis: A Review. Applied Sciences 2019, 9, 1345, doi:10.3390/app9071345.

[20] *Mallat, S.G.*: A theory for multiresolution signal decomposition: the wavelet representation. IEEE Trans. Pattern Anal. Machine Intell. 1989, 11, 674–693, doi:10.1109/34.192463.

[21] *Haqshenas, S.R.; Saffari, N.*: Multi-resolution analysis of passive cavitation detector signals. J. Phys.: Conf. Ser. 2015, 581, 12004, doi:10.1088/1742-6596/581/1/012004.

[22] *Cai, T.T.; Silverman, B.W.*: Incorporating Information on Neighbouring Coefficients into Wavelet Estimation. Sankhyā: The Indian Journal of Statistics, Series B (1960–2002) 2001, 63, 127–148.

Contacts

Dipl.-Ing. Karin Mascher, Graz University of Technology, Institute of Geodesy, Steyrergasse 30/III, 8010 Graz, Austria.
E-Mail: karin.mascher@tugraz.at

Univ.-Prof. Dipl.-Ing. Dr.techn. Philipp Berglez, Graz University of Technology, Institute of Geodesy, Working Group Navigation, Steyrergasse 30/II, 8010 Graz, Austria.
E-Mail: pberglez@tugraz.at